

Effect of binding to carbon black on the dynamics of 1,4-polybutadiene

J. H. Roh,^{1,a)} M. Tyagi,^{2,3} T. E. Hogan,⁴ and C. M. Roland^{1,b)}

¹Naval Research Laboratory, Chemistry Division, Code 6120, Washington, DC 20375-5342, USA

²National Institute of Standards and Technology, Center for Neutron Research, Gaithersburg, Maryland 20899-6100, USA

³Department of Materials Science and Engineering, University of Maryland, College Park, Maryland 20742, USA

⁴Bridgestone Americas, Center for Research and Technology, Akron, Ohio 44317-0001, USA

(Received 21 August 2013; accepted 13 September 2013; published online 3 October 2013)

The nature of the interactions of polymers at the surface of nanoparticles is crucial to understanding the dynamics and their relation to mechanical properties. The effect of binding (both chemical attachment and physical adsorption) on the local and global dynamics of chain molecules remains a controversial subject. Using neutron scattering and dynamic mechanical spectroscopies, we measured the slow conformational and terminal relaxations, as well as the fast local dynamics, of 1,4-polybutadiene (PBD) containing carbon black (CB) particles. We observed a substantial decrease in the flexibility of bound segments at temperatures through the glass transition temperature, T_g . The longer range motions of the PBD become more suppressed and cooperative as temperature decreases, while the relaxation time of the fast local dynamics is little affected by the CB particles. The mobile fraction of PBD is less sensitive to temperature when bound. Mechanical spectroscopy indicates that both the local segmental dynamics and the global chain modes are slowed by the filler. These results are consistent with transient structural arrest of the slow dynamics of atoms adjacent to the particles.
 © 2013 AIP Publishing LLC. [<http://dx.doi.org/10.1063/1.4822476>]

I. INTRODUCTION

Carbon black (CB) is the most widely used filler for reinforcing polymers, conferring improvements in mechanical properties and lowering material costs. CB particles vary in size from 17 to more than 100 nm, with the primary structures forming aggregates that are roughly twice as large.¹ Enormous effort has been expended to determine the physical nature of CB, particularly in rubbery polymers.² The interactions of polymer chains adjacent to CB are a key to understanding the dynamical and mechanical properties of these nanocomposites.³ Smaller particles, having greater specific surface area, emphasize the role of any bound polymer. Generally, the physical interactions and adsorption characteristics of carbon-based nanoparticles (CB, graphite, carbon nanotubes, graphene, diamond, etc.) and their effect on dynamical properties remain poorly understood.⁴ For example, distinctions are not made between chain segments immobilized by their spatial proximity to filler particles versus backbone units adsorbed at specific sites on the filler surface.³

Experimental studies have reached discordant conclusions concerning the effect of particle reinforcement on the local segmental dynamics.³ Reports of shifts of the glass transition temperature (T_g) due to filler-reinforcement sometimes have been based on changes in the frequency or temperature of the loss tangent peak in mechanical spectra.⁵ However, the position of this peak is also influenced by the magnitude of the storage modulus at lower frequencies (within the rubbery plateau), and since this is also affected by the

filler, shifts of the loss tangent do not necessarily reflect changes in the segmental dynamics.⁶ A highly cited work is that of Tsagaropoulos and Eisenberg,^{7,8} who observed additional loss peaks in silica-filled polymers at temperatures 100 °C above T_g of the bulk polymer, which they ascribed to a glassy phase of polymer in close proximity to the silica particles. However, it is not clear how such putative high temperature glass transition peaks can be distinguished from mechanical loss associated with terminal flow, which also is affected by filler interaction.⁹ NMR is a common tool to investigate polymer dynamics in nanoparticle composites, but fitting relatively featureless proton relaxation profiles can yield ambiguous results. Some NMR analyses^{4(a)–4(h)} suggest dramatic increases in the rigidity of polymers near T_g , while others conclude the mobility of the bound segments is unaffected or even greater than that for the unfilled polymer.^{4(i),10} Similarly divergent results have been obtained by dilatometry^{4(j)} and neutron scattering^{4(l)} for polyisoprene in the glassy state.

A satisfactory understanding of the dynamics of polymers in nanocomposites requires addressing the following issues: Does binding suppress the local dynamics of the polymer, and if so, which timescales are most affected? What governs the partitioning of segments into restricted and unaffected dynamic modes? How do the relaxation dynamics vary with temperature; in particular, is there a qualitative difference in the effect of the filler particles above and below T_g ? How do the macroscopic mechanical properties reflect the effect of nanoparticles on the chain dynamics? In this study, we investigate the dynamics in the pico- and nanosecond timescales of 1,4-polybutadiene (PBD) bound to CB

^{a)}National Research Council postdoctoral fellow.

^{b)}mike.roland@nrl.navy.mil. Telephone: 202-767-1719. Fax: 202-767-0594.

particles. We employ two neutron scattering techniques, in combination with dynamic mechanical measurements. Incoherent neutron scattering analysis is a powerful method to examine microscopic motions of hydrogen atoms in polymer nanocomposites, and some studies have been reported.^{40,11} The role of any “bound polymer” can be accentuated by extraction of the soluble polymer prior to the neutron measurements. Quasielastic scattering spectra were analysed to quantify the relaxation rate, mobile fraction, and the displacements of the polymer chains. The dynamic mechanical measurements yield information about the polymer dynamics on both the local and global scales.

We find that the dynamics of PBD can be characterized by two microscopic relaxations at times in the range $40 \text{ ps} < t < 2 \text{ ns}$. The slow mode of bound PBD becomes strongly retarded as temperature decreases. Temperature variations of the dynamic mechanical response of the segmental relaxation and terminal flow at temperatures down to below T_g also exhibit filler-induced restricted dynamics on the 10^{-6} – 10^2 s timescales. However, CB interactions exert little effect on the fast modes at any temperature. The bound polymer, of course, has the larger immobile fraction, while for both modes, the change in the mobile fraction due to the presence of CB is smaller on cooling toward T_g . The collective vibrations, prominent below T_g , show negligible effect of CB binding.

II. EXPERIMENT

The weight-averaged molar mass of PBD was 158 kD, with a polydispersity of 1.07. The chemical structure was butadiene 1,4-addition product with 14% vinyl groups (1,2-addition). The carbon black (Cabot Vulcan 9) was N110 (fused 17 nm particles); the mean diameter of the aggregates was about 54 nm.¹² The initial composition was 20.5 vol.% CB (33.3 wt.%). After being mixed on a two-roll mill, the compound was Soxhlet extracted⁴⁰ using cyclohexane for 5 days. The extracted mixture was dried under vacuum at RT for 3 days, followed by 1 day at 80 °C. The composition after extraction was 60 vol.% CB, as determined by thermogravimetry (TA Instruments Q500). Differential scanning calorimetry (TA Instruments Q100) was carried out at a 10 K/min heating rate to determine glass transition temperatures.

Neutron scattering measurements on neat PBD and the extracted nanocomposite employed the High-Flux Backscattering (HFBS, NG2) and Disk Chopper (DCS, NG4) spectrometers at NIST. The energy ranges were up to $E = 17 \mu\text{eV}$, with $0.4 \mu\text{eV}$ resolution defined by the half-width at half maximum of an elastic peak (0.24–4 GHz, 40 ps to 2 ns) for the HFBS, and up to $E = 20 \text{ meV}$ with a $25 \mu\text{eV}$ resolution (12 GHz to 4.8 THz, 0.03–26 ps) for the DCS. The range of the scattering vector was $0.31 \text{ \AA}^{-1} \leq Q \leq 1.71 \text{ \AA}^{-1}$ for HFBS and $0.2 \text{ \AA}^{-1} \leq Q \leq 2 \text{ \AA}^{-1}$ for DCS. The former was used for higher temperature measurements ($>240 \text{ K}$) to monitor segmental relaxation, and the latter for lower temperatures to follow the collective vibrational modes. Samples were contained in annular, aluminium holders, with thicknesses ($\sim 0.1 \text{ mm}$) sufficiently thin to avoid multiple scattering.

Dynamic shear moduli of neat PBD and the as-mixed PBD/CB compound were obtained over the frequency range 5×10^{-3} to 10 Hz using an Anton Paar MCR 502 rheometer. (After extraction the nanocomposite material lacked sufficient mechanical integrity for rheometry measurements.) The samples were disk-shaped, with a typical diameter around 10 mm and $\sim 0.5 \text{ mm}$ thickness, and measured using parallel plates. The frequency dependence of the shear modulus was obtained at $\sim 0.1\%$ strain amplitude at temperatures from 177 to 315 K.

III. RESULTS

A. Analysis of weight fraction, surface area, and T_g of the bound polymer

TGA analysis indicated that $26 \pm 0.4 \text{ wt.}\%$ polymer remained after extraction (see Figure 1 of the supplementary material¹³), which means the volume fraction of CB nanoparticles increased threefold. This agrees with general results of bound rubber for unsaturated polymers.⁴⁰ Based on the size of the CB particles and the radius of gyration of the PBD, we estimate that about 25% of the CB surface could be covered by the polymer;¹⁸ that is, all the chains are in close proximity to the particles and have at least one repeat unit bound to the CB. From DSC (see Figure 2 of the supplementary material¹³), the bound PBD has a T_g that is 1.3 K higher than the value for the neat rubber ($=180 \text{ K}$), and the transition is significantly broader. This presumably reflects the constraints from chemi- and strong physisorption of the chain segments.

B. Microscopic local dynamics: Slow and fast processes, and collective vibrations

The neutron scattering spectrum is dominated by incoherent scattering from hydrogen atoms, which contributes 94% of the total scattering for the PBD and 82% for the extracted nanocomposite. This means the quasielastic spectra primarily reflect the motions of the hydrogen atoms in the polymer. The temperature-dependent atomic mean-square-displacement

$$\langle r^2(T) \rangle = -3Q^{-2} \ln[I_{el}(Q, T)/I_{el}(Q, 4K)], \quad (1)$$

where I_{el} is the elastic neutron scattering intensity of HFBS, yields information about the damped local motions arising from segmental and secondary dynamics, and the collective vibrations. Figure 1 shows that anharmonic motions emerge in both the neat and bound rubber at temperatures around 180–200 K. Traditionally this is referred to as the dynamic transition temperature, T_d , because it demarcates the onset of conformational relaxation.^{14,15}

The deviation from a linear T -dependence in Figure 1 occurs over a broad range, with no large differences between the neat and filled polymer. However, the value of $\langle r^2 \rangle$ averaged over a range of Q is significantly smaller for the extracted mixture (about 1.7 times at 300 K) than for neat PBD, showing directly that the mobility of the chains is suppressed by interaction with the CB particles. As temperature decreases, this difference in magnitude of $\langle r^2 \rangle$ is reduced, with equivalent behavior below T_d . Since analysis of the mean-squared-displacement alone does not discriminate among the differ-

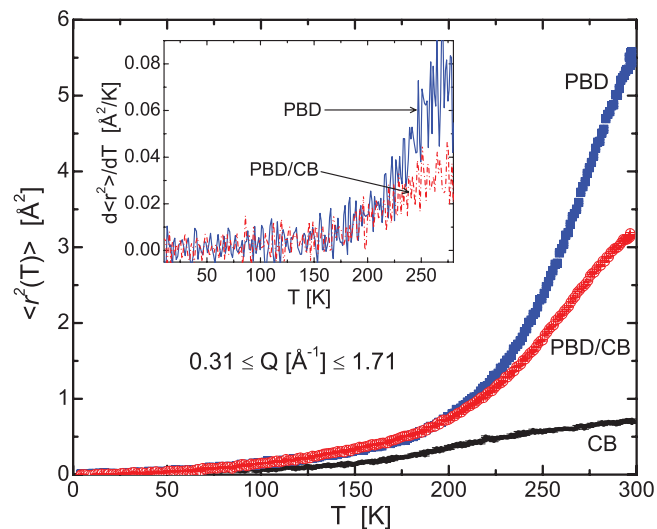


FIG. 1. Mean-square-displacement of hydrogen atoms for PBD, the nanocomposite, and the neat carbon black. Inset displays temperature derivatives of $\langle r^2(T) \rangle$.

ent dynamic modes, we measured energy-resolved neutron scattering spectra covering 0.03–26 ps for temperatures $\leq T_d$, and from 40 ps to 2 ns for higher temperatures.

Figure 2 shows the dynamic structure factors, $S(E)$, summed over all Q , for the neat PBD and the nanocomposite at several temperatures, and for the pure CB at 285 K. Greater broadening of the quasielastic spectrum indicates faster relaxation, a larger mobile fraction, and/or a larger length scale of the motions. There is negligible quasielastic scattering (QES)

from neat CB above the instrumental resolution, reflecting the absence of relaxation processes in the filler. Thus, the QES of the extracted PBD/CB can be interpreted in terms of motion of the hydrogen atoms of the bound polymer chains. Consistent with the $\langle r^2(T) \rangle$ results in Figure 1, the $S(E)$ of bound PBD shows lower QES intensity in the given energy window at all temperatures (240–300 K), although the difference is small at the lowest temperature.

The segmental relaxation dynamics of polymers generally conform to a Kohlrausch stretched exponential function,^{16,17} however, the limited spectral range of the data in Figure 2 makes such line-shape analysis difficult. In a previous communication¹⁸ we used dielectric and mechanical spectroscopies to determine the Kohlrausch parameters, and then employed these to characterize the QES data. We adopt a different approach herein in order to resolve multiple dynamic modes, analysing data over a broader frequency range that includes lower temperature measurements. As an approximation, we employ two Lorentzian functions to describe the QES. Our purpose is to monitor the fast and slow modes of the polymer, which in reality encompass a range of mobilities; however, their dynamics are sufficiently different to make such a categorization tenable. There is precedent for this method of extracting representative relaxation times for well resolved fast and slow modes,^{15(b),19} although higher time resolution measurements make clear that the actual spectra are broader than Lorentzian.²⁰ We fit the spectra to an equation representing the deconvolution of the total scattering spectrum into an elastic and two quasielastic functions, corresponding, respectively, to incoherent scattering of

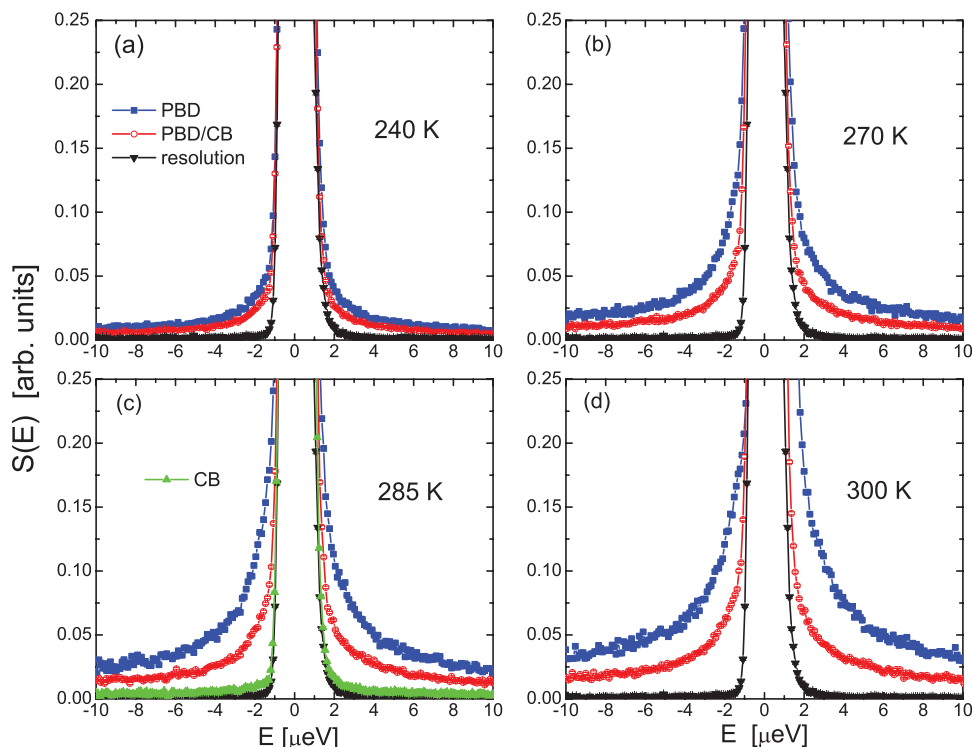


FIG. 2. Dynamic structure factor summed over all Q values ($0.31 \leq Q (\text{\AA}^{-1}) \leq 1.71$) for PBD, the nanocomposite, and at 285 K the neat CB. Also shown is the resolution function from $S(E)$ measured for PBD at 4 K, which provides completely elastic scattering.

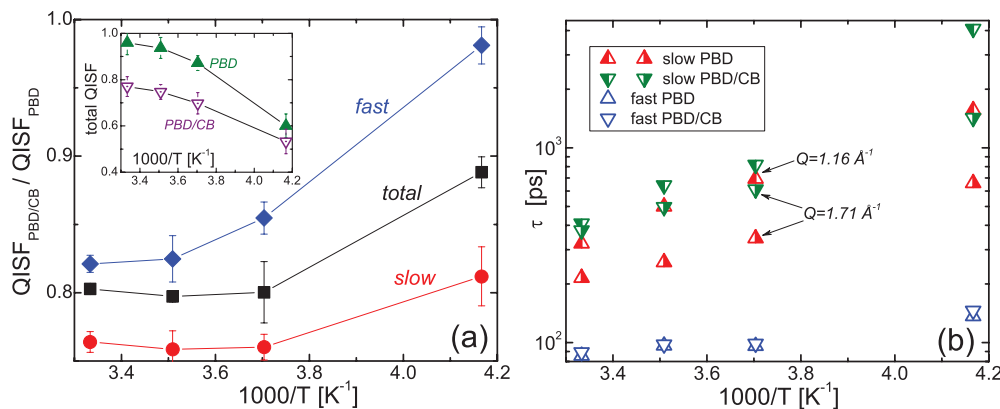


FIG. 3. Dynamic quantities from fit of Eqs. (1)–(3) to $S(Q, E)$. (a) Ratio of quasielastic incoherent structure factor for the nanocomposite to that for neat PBD. These QISF values were averaged for $Q \geq 1.16 \text{ \AA}^{-1}$. Inset shows the sum of $\text{QISF}_{\text{fast}}$ and $\text{QISF}_{\text{slow}}$ for the two samples. (b) Corresponding relaxation times, with values for the slow process determined at the two indicated scattering vectors; relaxation times for the fast mode showed no Q -dependence and the plotted τ_{fast} are the average for all $Q > 1.16 \text{ \AA}^{-1}$. For the filled PBD at the highest temperature (240 K), τ_{slow} is beyond the time resolution (~ 1660 ps); the approximate value was obtained after deconvolution of the resolution function (Eq. (2)). Error bars here and elsewhere represent one standard deviation.

an immobile and two relaxational (slow and fast) modes.^{15,19} In normalized form

$$\begin{aligned}
 S(Q, E) = & DW(Q)[EISF(Q)\delta(E) \\
 & + QISF_{\text{slow}}(Q)L_{\text{slow}}(\Gamma_{\text{slow}}(Q), E) \\
 & + QISF_{\text{fast}}(Q)L_{\text{fast}}(\Gamma_{\text{fast}}(Q), E)] \\
 & \otimes R(E), \quad (2)
 \end{aligned}$$

where \otimes signifies convolution, and

$$L(\Gamma(Q), E) = \pi^{-1} \frac{\Gamma(Q)}{E^2 + (\Gamma(Q))^2}. \quad (3)$$

The DW , L , Γ , and $R(E)$ are, respectively, the Debye-Waller factor, a Lorentzian function, the half-width at half-maximum of the QES peak, and a resolution function. (An example of this peak-shape analysis is shown in Figure 3 of the supplementary material¹³.) $EISF(Q)$ represents the elastic incoherent scattering factor. The quasielastic incoherent scattering factor (QISF) is obtained from the amplitudes and reflects the respective fractions of the slow and fast relaxation mode.

In principle the Q -dependent fit parameters obtained from the QES peak analysis provide information on the relaxation timescale, mobile fraction, and diffusion distance; however, the approximation of the relaxation spectra as Lorentzian limits the amount of quantitative information that can be extracted. Nevertheless, microscopic models of relaxation processes based on Lorentzian functions have been shown capable of providing at least qualitative interpretations of incoherent scattering from polymers.^{19(a),20,21}

Figure 3(a) shows the ratio of QISF for the bound rubber to that for neat PBD. The QISF is averaged over the Q range (1.16 – 1.71 \AA^{-1}) in which the total QISF has reached an asymptotic value. For both the slow and fast processes at all temperatures, QISF of the bound PBD is less than for the neat PBD. The ratio in Figure 3(a) is proportional to their relative mobilities, so these data show directly local immobilization in the nanocomposite. The QISF ratio is closer to unity for the fast process, increasing more strongly as temperature is low-

ered, indicating less restriction due to CB than for the slow mode.

The characteristic relaxation times of the two dynamic modes are plotted as a function of inverse temperature in Figure 3(b). The relaxation time for the slow process varies with Q , while τ_{fast} shows no significant dependence on scattering vector (and thus was averaged over all $Q > 0.5 \text{ \AA}^{-1}$). This Q -invariance is consistent with the fast process being more local, and thus less affected by proximity to the particles. As opposed to the slow process, the temperature variation of the relaxation time of the fast mode is largely unaffected by the CB at all temperature (Figure 3(b)).

Diffusion constants of the slow process, D_{slow} , were obtained by fitting a jump diffusion model²² to the Q -dependent half-widths to (see Figure 4 of the supplementary material¹³)

$$\Gamma_{\text{slow}}(Q) = \frac{D_{\text{slow}}Q^2}{1 + D_{\text{slow}}Q^2\tau_0}, \quad (4)$$

where τ_0 is the waiting time. Note that this analysis describes only local diffusion, given the limited temporal and spatial scales of the QES measurements. Similar to the trend of τ_{slow} (Figure 3(b)), the difference for D_{slow} between the bound and neat rubber becomes substantial (factor of ~ 2) at lower temperatures (Figure 4). The characteristic jump distance, defined from the diffusion constant as $L = \sqrt{6\tau_0 D_{\text{slow}}}$ and listed in Table I, shows no significant changes at temperatures ≥ 270 K, falling in the range 1.8 – 2.3 \AA . This magnitude is consistent with determinations of the length scale of monomer diffusion for 1,4 polybutadiene derived from scaling of the macroscopic viscosity with the interchain pair correlation function probed by neutron spin echo spectroscopy.²³ At 240 K there is insufficient diffusion over the available time window and Q values for an accurate analysis. The diffusion constant at such low temperature was estimated by assuming simple linear diffusion ($\Gamma(Q) = D_{\text{slow}}Q^2$),^{22(b),24} instead of Eq. (4). This assumption is justified because for such limited diffusion, τ_0 is small relative to the diffusion time.

Figure 5 shows the DCS dynamic structure factor summed over a Q range of $0.2 \text{ \AA}^{-1} \leq Q \leq 2 \text{ \AA}^{-1}$. Broadening of the QES and the boson peak is apparent in both samples at

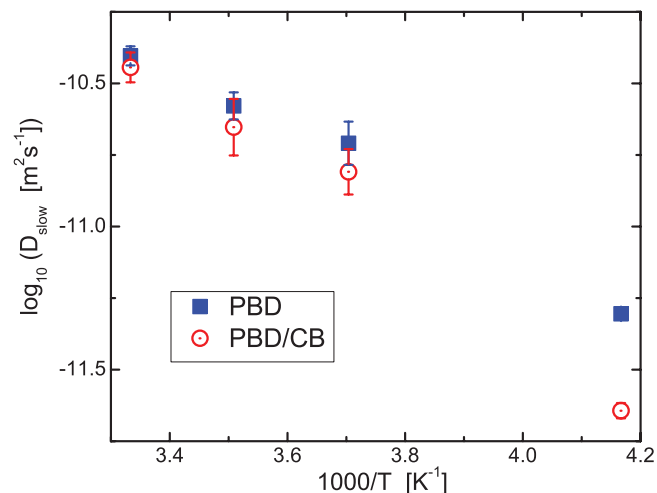


FIG. 4. Diffusion constant, D_{slow} , of neat and bound PBD, obtained from the QES half-widths using Eq. (4); the parameters are shown in Table I. These data do not represent absolute diffusion properties because of the limited energy and time resolution.

all sub- T_g temperatures; however, the dynamics of neat PBD shows greater intensity than for the filled sample. Similar to the HFBS results, the ratio of DCS-QISF (integrated in the energy range from 0.6 to 20 meV) of the bound to neat PBD increases as temperature decreases (Figure 5, inset). At 60 K, the number of mobile sites, which involve only the fast process and collective vibrations, is essentially equivalent for the neat polymer and the nanocomposite.

C. Dynamic mechanical results

Dynamic mechanical measurements between 177 and 315 K were carried out on the neat and filled PBD (the latter measured as prepared because the extracted material lacked the cohesiveness required for mechanical testing). The spectra are shown in Figure 5 of the supplementary material¹³. In Figure 6 are the relaxation times, defined from the frequency of the peak, $(2\pi\nu_{peak})^{-1}$, for the local segmental and global chain modes. The data for the neat polymer are consistent with literature results for polybutadienes having similar chemical structure.²⁵ At the shear strains employed ($\sim 0.1\%$), the nanocomposite exhibits no Payne effect;²⁶ i.e., the response was linear (Figure 6 of the supplementary material¹³). Even though the filled sample contains unattached PBD chains, both the local and global relaxation times are longer than for the neat PBD. The difference in dynamics between the neat PBD and the nanocomposite corresponds to about a 1 K difference in glass transition temperatures. This dif-

TABLE I. Jump diffusion model parameters (Eq. (4)).

Temperature (K)	300	285	270
τ_0 (ps) PBD	142 ± 16	214 ± 35	357 ± 50
τ_0 (ps) PBD/CB	254 ± 49	387 ± 67	647 ± 74
L (\AA) PBD	1.83	1.84	2.04
L (\AA) PBD/CB	2.34	2.27	2.45

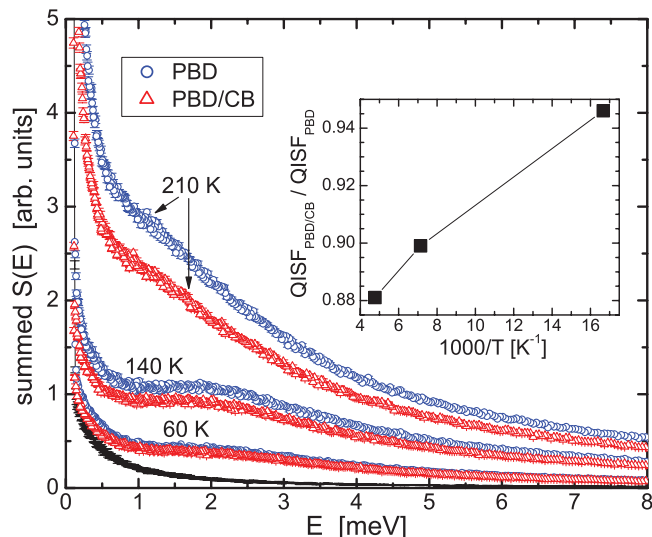


FIG. 5. Dynamic structure factor of DCS summed over the range $0.2 \leq Q$ (\AA^{-1}) ≤ 2 and normalized to the maximum elastic intensity of the resolution spectrum for PBD (circles) and the nanocomposite (triangles) at the indicated temperatures. The lowest curve is the resolution function, obtained as $S(E)$ of PBD at 2 K, for which the scattering is entirely elastic. Inset shows the ratio of QISF of the bound PBD to that of the neat polymer, for QISF obtained by integrating the QES intensity over the energy range, $0.6 \text{ meV} < E < 20 \text{ meV}$ after correction for the instrumental resolution.

ference in local segmental mobilities seen in the mechanical experiments is analogous to the observations for $\tau_{slow}(T)$ in Figure 3(b). The temperature dependences are non-Arrhenius behavior, with the only significant difference seen in the stronger effect of temperature changes on the global chain mode for the filled sample. The lines in Figure 6 are the fits of the Vogel-Fulcher-Tamman (VFT) equation,²⁷

$$\tau = \tau_{\infty} \exp\left(\frac{B}{T - T_0}\right), \quad (5)$$

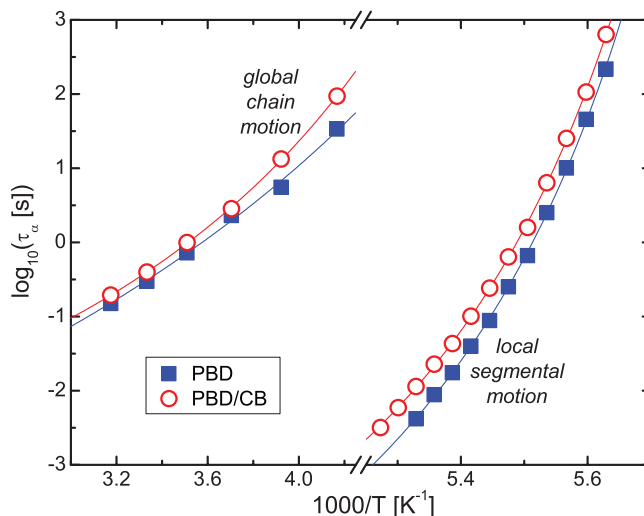


FIG. 6. Mechanical relaxation times for the terminal chain modes (upper curves) and local segmental dynamics (lower curves) for neat PBD (squares) and the CB nanocomposite (circles). Unlike the neutron scattering experiments, the latter was not extracted in order to have sufficient mechanical integrity for the measurements.

TABLE II. VFT fit parameters for mechanical relaxation times.

	Mode	$\log_{10}(\tau_{\infty} \text{ (s)})$	B (K)	T_0 (K)
PBD	Local segmental	-9.4 ± 0.4	401 ± 34	163 ± 1
PBD/CB ^a	Local segmental	-8.7 ± 0.2	371 ± 20	164 ± 1
PBD	Global chain	-4.5 ± 1.1	1611 ± 780	123 ± 35
PBD/CB ^a	Global chain	-3.7 ± 0.2	1089 ± 83	157 ± 4

^aUnextracted.

with the values obtained for the constants τ_{∞} , B, and T_0 tabulated in Table II.

IV. DISCUSSION

By employing an approximate analysis (Eq. (2)) necessitated by the limited time resolution, we identify two relaxation modes (slow and fast) in both bound and neat PBD, falling in the intermediate time range 40 ps to 2 ns. There is ample precedent for an analysis limited to two relaxation modes: NMR results^{4(a)–4(h)} have been interpreted as reflecting two dynamic processes, the slower constrained in the bound polymer layer at $T > T_g$, but no difference in the relaxation dynamics for the fast mode. By connecting the intermediate scattering functions obtained from neutron spin echo measurements of neat PBD in the range 3.5 ps $< t < 1.4$ ns and the viscosity at 100 $\mu\text{s} < t < 100$ s, Richter *et al.*^{15(a)} resolved two relaxations that were decoupled at $T > T_c$. More recently, Kanaya *et al.*^{15(b)} observed the presence of a localized motion, which he termed the E-process, in the time window of 20–400 ps at $T > T_c$. This E-process, attributed to isolated conformational transitions in the tens of picosecond timescale at room temperature, was unaffected by intermolecular cooperativity.^{15(b),28} The slow and fast processes herein exhibit temperature dependences consistent with those reported by Kanaya *et al.*^{15(b)}

Richter *et al.*²³ determined that the jump length of monomeric diffusion involving structural relaxation is around 2 Å; this agrees well with our result, $L \sim 2\text{--}2.5$ Å for $T \geq 270$ K. This jump length pertains to the slow process of the bound rubber at higher temperatures, and is about 25% larger than for neat PBD, with a waiting time that is 1.8 times longer (Table I). The decreases for the slow dynamic mode of its relaxation rate by a factor of 2–2.6 (Figure 3(b)) and diffusion constant by ~ 2.3 times (Figure 4) are accentuated at lower temperatures (240 K).

Our QES experiments probe only atoms exhibiting mobility within a relatively narrow energy range, so that PBD segments chemisorbed onto the particles are clearly evident. However, repeat units adjacent to tethered segments, that is, within the correlation length of the slow process, will also experience slower dynamics. Additionally, “transient locking,” whereby atoms are reversibly adsorbed at the CB surface, will manifest as retarded dynamics. The substantial increase in the waiting time without change in jump distance (Table I) is consistent with a model of particle interactions involving such transient arrest of the chain segments.

In contrast to most studies, neutron scattering experiments with higher energy resolution⁴⁽ⁱ⁾ reported that the mo-

bility of polyisoprene, defined by the breadth of the peak in the density of states at ~ 25 meV, increased by ~ 1 meV below T_g in CB nanocomposites. However, a larger intensity of the density of states was found in the neat polymer, suggesting that the bound polymer has fewer mobile groups. This is similar to our sub- T_g DCS results (Figure 5). Since the reinforcing mechanism for carbon black involves hydrogen atoms from the polymer interacting at the surface of the particle,² interference from rapid reorientation of the pendant methyl groups on the polyisoprene chain (analogous to the fast modes that are unaffected by the CB) may lead to less constraint on the dynamics, and hence the qualitatively different effect of carbon black on polyisoprene in comparison to the present results for PBD.

V. SUMMARY

Quasielastic neutron scattering experiments comparing CB-filled and neat PBD demonstrate differences in microscopic relaxation rates, with partitioning of the dynamics between fast and slow modes. In contrast to a previous inelastic neutron scattering study on polyisoprene,⁴⁽ⁱ⁾ we find no indication of greater mobility of the polybutadiene due to confinement or other interaction with CB in the 0.03 ps to 2 ns time span at temperatures encompassing the glass transition. Rather we find that the local rigidity of PBD increases for temperatures above the dynamic transition temperature. The relaxation of the more localized fast dynamics is relatively unaffected by the CB, while interaction with CB hinders the slow dynamics, especially at lower temperatures. Supporting our neutron scattering results, dynamic mechanical measurements show that the segmental dynamics and the terminal chain modes are both slower in the nanocomposite.

ACKNOWLEDGMENTS

J.H.R. acknowledges a National Research Council-Naval Research Laboratory postdoctoral fellowship. This work was supported in part by the Office of Naval Research and utilized facilities supported in part by the National Science Foundation under Agreement No. DMR-0944772. The identification of commercial products does not imply endorsement by the National Institute of Standards and Technology nor does it imply that these are the best for the purpose.

¹C. G. Robertson, R. Bogoslovov, and C. M. Roland, *Phys. Rev. E* **75**, 051403 (2007).

²*Carbon Black, Science and Technology*, 2nd ed., edited by J.-B. Donnet, R. C. Bansal, and M.-J. Wang (Marcel Dekker, Inc., New York, 1993); *Polymer Nanocomposites*, edited by Y.-W. Mai and Z.-Z. Yu (Woodhead Publishing Ltd., Cambridge, 2006); T. A. Vilgis, G. Heinrich, and M. Klüppel, *Reinforcement of Polymer Nano-Composites: Theory, Experiments and Applications* (Cambridge University Press, 2009).

³C. G. Robertson and C. M. Roland, *Rubber Chem. Technol.* **81**, 506–522 (2008), and references therein.

⁴(a) J. O’Brien, E. Cashell, G. E. Wardell, and V. J. McBrierty, *Macromolecules* **9**, 653–660 (1976); (b) J. C. Kenny, V. J. McBrierty, Z. Rigbi, and D. C. Douglass, *ibid.* **24**, 436–443 (1991); (c) H. Serizawa, T. Nakamura, I. K. Tanaka, and A. Nomura, *Polym. J.* **15**, 201–206 (1983); (d) C. R. Dybowski and R. W. Vaughan, *Macromolecules* **8**, 50–54 (1975); (e) N. K. Dutta, N. R. Choudhury, B. Haidar, A. Vidal, J. B. Donnet, L. Delmotte, and J. M. Chezeau, *Polymer* **35**, 4293–4299 (1994);

- (f) J. P. Cohen Addad and P. Frébourg, *ibid.* **37**, 4235–4242 (1996); (g) H. Lüchow, E. Breier, and W. Gronski, *Rubber Chem. Technol.* **70**, 747–758 (1997); (h) N. Kida, M. Ito, F. Yatsuyaygi, and H. Kaido, *J. Appl. Polym. Sci.* **61**, 1345–1350 (1996); (i) V. M. Litvinov and P. A. M. Steeman, *Macromolecules* **32**, 8476–8490 (1999); (j) G. Kraus and J. T. Gruver, *J. Polym. Sci., Part A-2* **8**, 571–581 (1970); (k) P. P. A. Smit, *Rheol. Acta* **8**, 277–287 (1969); (l) A. I. Nakatani, R. Ivkov, P. Papanek, H. Yang, and M. Gerspacher, *Rubber Chem. Technol.* **73**, 847–863 (2000).
- ⁵A. R. Greenberg, *J. Mater. Sci. Lett.* **6**, 78–80 (1987); J. Berriot, H. Montes, F. Lequeux, D. Long, and P. Sotta, *Macromolecules* **35**, 9756–9762 (2002).
- ⁶C. G. Robertson, C. J. Lin, M. Rackaitis, and C. M. Roland, *Macromolecules* **41**, 2727–2731 (2008).
- ⁷G. Tsagaropoulos and A. Eisenberg, *Macromolecules* **28**, 396–398 (1995).
- ⁸G. Tsagaropoulos and A. Eisenberg, *Macromolecules* **28**, 6067–6077 (1995).
- ⁹C. G. Robertson and M. Rackaitis, *Macromolecules* **44**, 1177–1181 (2011).
- ¹⁰J. Leisen, J. Breidt, and J. Kelm, *Rubber Chem. Technol.* **72**, 1–14 (1999); W. Hu, M. D. Ellul, A. H. Tsou, and S. Datta, *ibid.* **80**, 1–13 (2007).
- ¹¹S. Gagliardi, V. Arrighi, R. Ferguson, and M. T. F. Telling, *Physica B* **301**, 110–114 (2001); V. Arrighi, J. S. Higgins, A. N. Burgess, and G. Floudas, *Polymer* **39**, 6369–6376 (1998); A. Triolo, F. Lo Celso, F. Negroni, V. Arrighi, H. Qian, R. E. Lechner, A. Desmedt, J. Peiper, B. Frick, and R. Triolo, *Appl. Phys. A* **74**, S490–S492 (2002).
- ¹²W. M. Hess and G. C. McDonald, *Rubber Chem. Technol.* **56**, 892–917 (1983).
- ¹³See supplementary material at <http://dx.doi.org/10.1063/1.4822476> for figures of thermogravimetric analysis, differential scanning calorimetry analysis, representative fit of two Lorentzian functions to a quasielastic peak of HFBS, Q^2 -dependent of full width of half maximum of the Lorentzian function associated with slow relaxation, and dynamic mechanical analysis of segmental and terminal relaxation.
- ¹⁴C. M. Roland and K. L. Ngai, *J. Chem. Phys.* **104**, 2967–2970 (1996).
- ¹⁵(a) D. Richter, R. Zorn, B. Farago, B. Frick, and L. J. Fetters, *Phys. Rev. Lett.* **68**, 71–74 (1992); (b) T. Kanaya, T. Kawaguchi, and K. Kaji, *Macromolecules* **32**, 1672–1678 (1999).
- ¹⁶F. Kohlrausch, *Pogg Ann. Phys.* **119**, 352 (1863).
- ¹⁷G. Williams and D. C. Watts, *Trans. Faraday Soc.* **66**, 80 (1970).
- ¹⁸J. H. Roh, M. Tyagi, T. E. Hogan, and C. M. Roland, *Macromolecules* **46**, 6667–6669 (2013).
- ¹⁹(a) M. Kofu, T. Someya, S. Tatsumi, K. Ueno, T. Ueki, M. Watanabe, T. Matsunaga, M. Shibayama, V. Garcia Sakai, and M. Tyagi, *Soft Matter* **8**, 7888–7897 (2012); (b) W. Zajac, B. J. Gabrys, R. McGreevy, and B. Mattssons, *Physica B* **226**, 144–151 (1996); (c) C. Smuda, S. Busch, G. Gemmecker, and T. Unruh, *J. Chem. Phys.* **129**, 014513 (2008); (d) T. Unruh, C. Smuda, S. Busch, J. Neuhaus, and W. Petry, *ibid.* **129**, 121106 (2008).
- ²⁰S. Khodadadi, S. Pawlus, J. H. Roh, V. G. Sakai, E. Mamontov, and A. P. Sokolov, *J. Chem. Phys.* **128**, 195106-1–195106-5 (2008); J. H. Roh, M. Tyagi, R. M. Briber, S. A. Woodson, and A. P. Sokolov, *J. Am. Chem. Soc.* **133**, 16406–16409 (2011).
- ²¹G. Paradossi, F. Cavalieri, E. Chiessi, and M. T. F. Telling, *J. Phys. Chem. B* **107**, 8363–8371 (2003); A. Nogales, T. A. Ezquerro, F. Batallán, B. Frick, E. López-Cabarcos, and J. Baltá-Calleja, *Macromolecules* **32**, 2301–2308 (1999); M. Bée, *Quasielastic Neutron Scattering: Principles and Applications in Solid State Chemistry, Biology, and Materials Science* (Adam Hilger, Bristol, 1988); *Chem. Phys.* **292**, 121–141 (2003); P. D. Hong, W. T. Chuang, W. J. Yeh, and T.-L. Lin, *Polymer* **43**, 6879–6886 (2002); A. Arbe and J. Colmenero, *Phys. Rev. E* **80**, 041805-1–041805-13 (2009); S. Lyonnard, Q. Berrod, B. A. Bruning, G. Gebel, A. Guillermo, H. Ftouni, J. Ollivier, and B. Frick, *Eur. Phys. J. Spec. Top.* **189**, 205–216 (2010); A. Sanz, T. A. Ezquerro, M. C. García-Gutiérrez, I. Puenta-Orench, J. Campo, and A. Nogales, *Eur. Phys. J. E* **36**, 24–32 (2013).
- ²²(a) T. Kanaya, K. Kaji, and K. Inoue, *Macromolecules* **24**, 1826–1832 (1991); (b) R. Lefort, D. Morineau, R. Guégan, C. Ecolivet, M. Guendouz, J.-M. Zanotti, and B. Frick, *Phys. Chem. Chem. Phys.* **10**, 2993–2999 (2008).
- ²³D. Richter, B. Frick, and B. Farago, *Phys. Rev. Lett.* **61**, 2465–2468 (1988).
- ²⁴C. Talon, L. J. Smith, J. W. Brady, B. A. Lewis, J. R. D. Copley, D. L. Price, and M.-L. Saboungi, *J. Phys. Chem. B* **108**, 5120–5126 (2004); L. J. Smith, D. L. Price, Z. Chowdhuri, J. W. Brady, and M.-L. Saboungi, *J. Chem. Phys.* **120**, 3527–3530 (2004); K. Wood, C. Caronna, P. Fouquet, W. Hausler, F. Natali, J. Ollivier, A. Orecchini, M. Plazanet, and G. Zaccai, *Chem. Phys.* **345**, 305–314 (2008); A. Meyer, S. Stuber, D. Holland-Moritz, O. Heinen, and T. Unruh, *Phys. Rev. B* **77**, 092201 (2008).
- ²⁵C. M. Roland and K. L. Ngai, *Macromolecules* **24**, 5315–5319 (1991); R. Zorn, F. I. Mopsik, G. B. McKenna, L. Willner, and D. Richter, *J. Chem. Phys.* **107**, 3645–3655 (1997); R. Casalini, K. L. Ngai, C. G. Robertson, and C. M. Roland, *J. Polym. Sci. Polym. Phys. Ed.* **38**, 1841–1847 (2000); C. G. Robertson and C. M. Rademacher, *Macromolecules* **37**, 10009–10017 (2004); R. B. Bogoslovov, T. E. Hogan, and C. M. Roland, *ibid.* **43**, 2904–2909 (2010).
- ²⁶C. M. Roland, *J. Rheol.* **34**, 25–34 (1990); X. Wang and C. G. Robertson, *Phys. Rev. E* **72**, 031406 (2005).
- ²⁷C. M. Roland, *Viscoelastic Behavior of Rubbery Materials* (Oxford University Press, Oxford, 2011).
- ²⁸R. H. Gee and R. H. Boyd, *J. Chem. Phys.* **101**, 8028–8038 (1994); E.-G. Kim and W. L. Mattice, *ibid.* **101**, 6242–6254 (1994).